Indian Journal of Pure & Applied Physics
Vol. 53, October 2015, pp. 701-704

# Magnetization reversal of transition metal doped ZnO nanosystems

Trisha Mondal, Ajay Tripathi & Archana Tiwari*

Department of Physics, School of Physical Sciences, Sikkim University, Gangtok, Sikkim 737 102, India

*E-mail: archana.tiwari.ox@gmail.com

*Received 30 September 2014; revised 22 April 2015; accepted 20 August 2015*

Magnetization reversal of magnetic moments in transition metal ions doped ZnO nanosystems has been studied in the present paper. Stoner-Wohlfarth model is used to illustrate the energy surfaces, magnetic hysteresis and the coherent switching behaviour of magnetic moments. Low magnetic anisotropy in $Zn_{1-x}M_xO$ (M=Fe, Co, Ni) nanosystems is observed for various concentrations (x) of the doped ions. The anisotropies of $Zn_{1-x}M_xO$ when synthesized by three different techniques viz. chemical precipitation, pulsed laser deposition and sol-gel, have been compared. The temporal reversal paths of $Zn_{1-x}M_xO$ magnetic moments are elucidated and their switching times are reported.

**Keywords:** Magnetization, Magnetic moments**,** Nanosystems, Magnetic hysteresis

## 1 Introduction

In magnetic storage devices, information is stored in the orientations of magnetic moments and can be manipulated using the reversal processes[1,2]. For high density magnetic recording media, thermal stability with negligible media noise, scalable films with perpendicular magnetic anisotropies, and non-zero coercive fields are desirable[3,4]. The storage density can be enhanced by miniaturizing the grain size of magnetic particles. Smaller grains, though reduce the media noise, cause thermal instability. One may control the thermal instability by using materials with larger magnetic anisotropy[5].

Oxide-diluted magnetic semiconductors (oxide-DMS) have attracted much interest in recent years in the field of magnetic recording and spintronic devices[6-8]. Transition metals (TM) doped ZnO matrices show room temperature ferromagnetism and could be potentially used towards data storage and recording purpose[9,10]. Ferromagnetic properties of TM-DMSs are exhaustively investigated both theoretically as well as experimentally. However, these studies show disparity in elucidating the origin of room temperature ferromagnetism[11-13] in the DMSs.

Stoner-Wohlfarth (SW) model, which relates magnetic hysteresis to the coherent rotation of the moments in anisotropic materials, is widely used for evaluating the magnetic properties of ferromagnets[14]. In particular, it links the switching field to the macroscopic coercivity and physical properties of the material such as its composition, crystal structure and shape. Fast dynamic responses of magnetization can be used for high-speed information recording and processing purpose[15]. Time reversal path of magnetization $M$ can be illustrated by Landau-Lifschitz (LL) equation where the damping coefficient $\alpha$ is used to illustrate magnetization precession around the applied magnetic field. In thin-films, $\alpha$ depends significantly on methods of sample preparation and its topology[16].

In the present paper, magnetization and its reversal in ZnO nanosystems have been studied. SW model is used to demonstrate the switching behaviour of magnetic moments by observing their energy surfaces and the hysteresis. The switching fields and effective anisotropy are compared for $Zn_{1-x}M_xO$ for various kinds (M) and concentrations (x) of the dopants. The time evolution for the magnetic moment in different TM-doped ZnO has been studied in order to find suitable device for high speed information recording and processing.

## 2 Materials and Methods

Our results are partly based on SW model which uses saturation magnetization, $M_s$ and coercive field, $H_c$ given in the earlier experimental reports. Three different methods of synthesis of $Zn_{1-x}M_xO$ (M=Fe, Co, Ni) are considered viz. chemical precipitation[17], pulsed laser deposition[18-21] (PLD) and sol-gel technique[16,22,23]. Nanopowders are synthesized by the chemical precipitation technique whereas PLD yields

nanofilms. The sol-gel technique produces both nano powders as well as thin films.

In the present paper the switching field ($H_s$) and effective anisotropy ($K_{eff}$) are compared for nano powders and thin films of $Zn_{1-x}M_xO$ with similar concentrations. The $M_s$ and $H_c$ values for respective methods are given in Table 1. In chemical precipitation technique, the samples were prepared for 2% and 5% dopants. However, $M_s$ and $H_c$ values are only been reported for 2% of the dopants in the matrix[17]. The given parameters have been used to evaluate $H_c$ for the matrices with 5% dopants. Both experimental and calculated $M_s$ and $H_c$ values of ZnO matrices for 2%, 4% and 5% dopants synthesized by the three techniques are tabulated in Table 1.

## 3 Results and Discussion

### 3.1 Stoner–Wohlfarth Model

The total energy needed to reverse the magnetic moment is the sum of effective anisotropy energy and the Zeeman energy due to external magnetic field. The energy density can be written as:

$$E(\theta)=\sin^2(\varphi-\theta)-h\cos\theta \quad \ldots(1)$$

where θ is the angle between magnetization $M$ and applied magnetic field $H$, $h = H/H_K$ is a constant for an angle φ between $H$ and the easy axis, $H_K$ is the anisotropy field and $K_{eff}$ is the effective anisotropy energy density given by $\mu_0 M_s H_K/2$. Effective anisotropy energy includes magneto-crystalline anisotropy and shape anisotropy[25]. Shape anisotropy of an ellipsoid magnetic grain, which arises due to demagnetization energy, is considered under uniaxial anisotropy[26]. At equilibrium, magnetization points along a direction defined by particular θ that minimizes the energy. For certain values of applied magnetic field, two energy minima are obtained which are considered for plotting the hysteresis curves.

In thin-films based magnetic recording media, a small region on the film stores the information. The dipolar field experienced by one of these small regions due to its neighbourhood is small if the easy axis is perpendicular to the film plane[5,27]. However, for φ=90°, no magnetic hysteresis is observed in $Zn_{1-x}M_xO$. In this paper, φ=85° is considered in order to reproduce the experimental hysteresis.

Table 1 — $M_s$ and $H_c$ values for 2%, 4% and 5% of metal ion (M) in $Zn_{1-x}M_xO$ when synthesized by chemical precipitation, PLD and sol-gel techniques

| Method | M | X | $M_s$ (A/m) | $H_c$ (A/m) | Ref. |
|---|---|---|---|---|---|
| | Fe | 2% | 7.5 | $2.1(\pm0.02)\times10^4$ | [17] |
| | | 5% | 50.4 | $3.2(\pm0.02)\times10^4$ | This work |
| Chemical | Co | 2% | 2.2 | $4.0(\pm0.1)\times10^3$ | [17] |
| precipitation | | 5% | 3.1 | $3.0(\pm0.1)\times10^3$ | This work |
| | Ni | 2% | 1.3 | $7.5(\pm0.1)\times10^3$ | [17] |
| | | 5% | 4.5 | $2.0(\pm0.1)\times10^4$ | This work |
| | Fe | 4% | $1.9\times10^3$ | $3.2\times10^3$ | [19] |
| PLD | Co | 5% | $4.1\times10^4$ | $2.0\times10^3$ | [18] |
| | Ni | 5% | $7.5\times10^3$ | $6.3\times10^3$ | [20] |
| Sol-gel | Fe | 5% | $1.5\times10^2$ | $1.23(\pm0.04)\times10^4$ | [22] |
| | Co | 5% | $3.5\times10^2$ | $7.2\times10^3$ | [24] |
| | Ni | 5% | $1.6\times10^3$ | $1.54\times10^4$ | [16] |

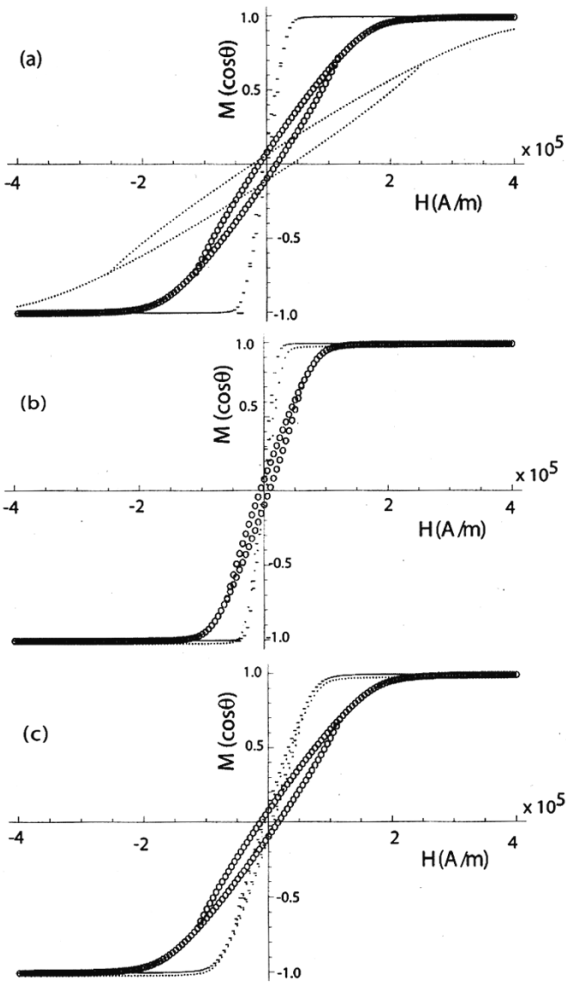


Fig. 1 — Hysteresis curve of (a) $Zn_{1-x}Fe_xO$ (b) $Zn_{1-x}Co_xO$ (c) $Zn_{1-x}Ni_xO$ where $x$ = 4% for $Zn_{1-x}Fe_xO$ when synthesized by PLD technique. For the remaining samples, $x$ = 5%. Dotted line corresponds to chemical precipitation, crossed squares corresponds to PLD and open circle corresponds to sol-gel synthesis

The hysteresis for $Zn_{0.96}Fe_{0.04}O$, $Zn_{0.95}Co_{0.05}O$ and $Zn_{0.95}Ni_{0.05}O$ are shown in Fig. 1 which are plotted by considering $M_s$ and $H_c$ given in Table 1. The hysteresis curves for $Zn_{1-x}M_xO$ drawn by using SW model are found identical to those of the experimental data. $H_K$ is calculated from the energy density equation and is used to evaluate the switching field[28,29] $H_s$ for $Zn_{1-x}M_xO$. The calculated $H_K$ and $H_s$ for $Zn_{1-x}M_xO$ are listed in Table 2 for both 2% and 5% dopants.

The grain size of $Zn_{1-x}M_xO$ nanoparticles prepared by chemical precipitation technique is about 7 nm, whereas for nano films synthesized by PLD and sol-gel techniques, it is about 30 and 17 nm, respectively[17,19]. Pertaining to their smaller and similar sizes, $Zn_{1-x}M_xO$ prepared by chemical precipitation and sol-gel techniques not only yield similar hysteresis curves but also require larger $H_s$ to reverse the magnetization as compared to when prepared by PLD technique.

The effective anisotropy energy density $K_{eff}$ is calculated using $H_K$ and $M_s$ for $Zn_{1-x}M_xO$ for $x$= 2%, 4% and 5% and are tabulated in Table 2. $K_{eff}$ is found to be of the order of $10^{-2}$-$10^2$ J/m$^3$ which is smaller as compared to those of the bulk metals (~$10^4$J/m$^3$). In DMSs synthesized by the chemical precipitation technique, $K_{eff}$ is found to be smaller than that of samples prepared by PLD and sol-gel techniques. It is also observed from Table 2 that for similar concentrations of the metal ion in ZnO matrices, the anisotropy varies with the synthesis techniques.

Effective magnetic anisotropy should be large for a thermally stable recording medium[5,30]. Due to the presence of relatively larger anisotropy, it is proposed that $Zn_{1-x}M_xO$ films prepared by PLD and/or sol-gel techniques can be used as thermally stable recording media for memory storage devices.

### 3.2 Dynamics of Magnetization: Magnetization Reversal

To evaluate the orientation of magnetization $M$ with respect to time, LL equation[31]:

$$M^2 \frac{d\vec{M}}{d\tau} = M(\vec{M} \times \vec{H}_{\text{eff}}) - \alpha[\vec{M} \times (\vec{M} \times \vec{H}_{\text{eff}})] \quad \ldots(2)$$

is used; $\tau$ is related to the time $t$ where $\tau = tM\gamma/(1+\alpha^2)$. $\alpha$ is the damping constant given by $\alpha=4\pi\nu/\gamma M_s$, $\nu$ is the relaxation frequency of moments and $\gamma$ is the gyromagnetic ratio[32]. The magnetization variation with time is obtained by solving LL equation for different instances of time. $M$ (0, 0.001, 1) in A/m are considered as initial conditions. Constant effective magnetic field ($H_{eff}$) of 1 A/m is applied in negative z-direction. The reversal of magnetization ($M_z$) as the function of time ($\tau$) in $Zn_{0.96}Fe_{0.04}O$, $Zn_{0.95}Co_{0.05}O$ and $Zn_{0.95}Ni_{0.05}O$ is plotted in Fig. 2. The time required for reversal of magnetization depends on the damping coefficient of the material.

$Zn_{1-x}M_xO$ prepared by PLD technique produces uniform thin films with larger $K_{eff}$. This is why, we have used their parameters to evaluate $\alpha$ and the time of magnetization reversal from one stable orientation to other. Relaxation frequencies are calculated from the line width of EPR (electron paramagnetic resonance) signal[33,34] ($\Delta H_{pp}$). In $Zn_{1-x}M_xO$ [M=Fe, Co, Ni], the EPR signal is attributed to $Fe^{2+}$, $Co^{2+}$ and $Ni^{2+}$ ions, respectively[35,36]. At room temperature, the line widths of EPR transitions are significantly influenced by the spin-lattice relaxation frequencies[37,38]. Using the relaxation frequencies for $Zn_{1-x}M_xO$, their $\alpha$ and the reversal time $\tau$ are calculated. The values of $\alpha$ and $\tau$ of $Zn_{1-x}M_xO$ moments are given in Table 3.

Figure 2 shows that the temporal switching of the magnetization $M_z$ in $Zn_{0.96}Fe_{0.04}O$ from one direction

Table 2 — $H_K$,$H_s$ and $K_{eff}$ for $\varphi = 85°$ of $Zn_{1-x}M_xO$ when synthesized by chemical precipitation, PLD and sol-gel techniques

| Method | Sample | $H_K$ (A/m) | $H_s$(A/m) | $K_{eff}$ (J/m$^3$) |
|---|---|---|---|---|
| Chemical precipitation | $Zn_{0.95}Fe_{0.05}O$ | $1.8\times10^5$ | $1.4\times10^5$ | 5.75 |
| | $Zn_{0.95}Co_{0.05}O$ | $1.6\times10^4$ | $1.2\times10^5$ | $3.2\times10^{-2}$ |
| | $Zn_{0.95}Ni_{0.05}O$ | $1.2\times10^4$ | $9.2\times10^4$ | $3.3\times10^{-2}$ |
| PLD | $Zn_{0.96}Fe_{0.04}O$ | $1.8\times10^4$ | $1.4\times10^4$ | $0.22\times10^2$ |
| | $Zn_{0.95}Co_{0.05}O$ | $1.2\times10^4$ | $9.2\times10^3$ | $3.06\times10^2$ |
| | $Zn_{0.95}Ni_{0.05}O$ | $3.8\times10^4$ | $2.9\times10^4$ | $1.81\times10^2$ |
| Sol-gel | $Zn_{0.95}Fe_{0.05}O$ | $8.2\times10^4$ | $6.3\times10^4$ | 7.73 |
| | $Zn_{0.95}Co_{0.05}O$ | $4.2\times10^4$ | $3.2\times10^4$ | 9.52 |
| | $Zn_{0.95}Ni_{0.05}O$ | $8.3\times10^4$ | $6.4\times10^4$ | 83.7 |

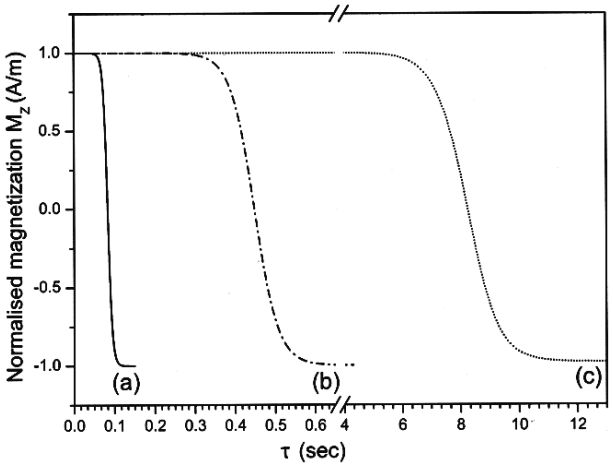


Fig. 2 — Magnetization reversal path with time in (a) $Zn_{0.96}Fe_{0.04}O$, (b) $Zn_{0.95}Ni_{0.05}O$ and (c) $Zn_{0.95}Co_{0.05}O$. For clarity, a break has been shown in time scale

Table 3 — Damping coefficient (α) and the switching time (τ) of $Zn_{1-x}M_xO$synthesized by PLD technique

| $Zn_{1-x}M_xO$ | $\Delta H_{pp}$ (G) | $M_s$ (A/m) | A | τ (ms) |
|---|---|---|---|---|
| $Zn_{0.96}Fe_{0.04}O$ | 1074.5 | $1.9 \times 10^3$ | 90 | 50 |
| $Zn_{0.95}Co_{0.05}O$ | 238.8 | $4 \times 10^4$ | 1 | 6400 |
| $Zn_{0.95}Ni_{0.05}O$ | 801.4 | $7.5 \times 10^3$ | 17 | 350 |

to the opposite one is faster than the other DMSs. The switching of magnetization in $Zn_{0.96}Co_{0.05}O$ takes relatively longer time. The quick magnetization reversal in $Zn_{0.96}Fe_{0.04}O$ makes it a potential system for realizing a faster magnetic switching and recording device.

## 4 Conclusions

Using a simplified SW model, we have explained the presence of room temperature ferromagnetism in ZnO DMSs. Our results suggest that preparatory techniques affect the shape and size of synthesized $Zn_{1-x}M_xO$ which in turn affects the system anisotropy. Anisotropy energy in $Zn_{1-x}M_xO$ is notably smaller than those reported for the bulk transition metals (M). Consequent changes in the total energy of these nano systems lead to smaller coercive field and weak ferromagnetic properties at room temperature. Time evolution of magnetic moment is observed for Fe, Co, Ni doped ZnO nanofilms. Maximum damping parameter is reported for $Zn_{0.96}Fe_{0.04}O$ which leads to a faster magnetization reversal. This is why, $Zn_{1-x}Fe_xO$, when synthesized by PLD technique, could be potentially used as a medium for magnetic data storage and recording purposes.

## Acknowledgement

Authors thankfully acknowledge UGC-DAE-CSR Indore for their support.

## References

1 Chappert C, Fert A & Dau F N Van, *Nature Materials,* 6 (2007) 813.
2 Vicario Carlo, Ruchert Clemens, Ardana-Lamas Fernando, Der-let Peter M, Tudu B, Luning Jan & Hauri Christoph P, *Nature Photonics,* 7 (2013) 720.
3 Ostler T A, Barker J, Evans R F L, Chantrell R W, Atxitia U, Chubykalo-Fesenko O, Moussaoui S El, Guyader L Le, Mengotti E & Heyderman L J, *Nature Communications*, 3 (2012) 666.
4 Ouari Bachir, Titov Serguey V, Mrabti Halim El & Kalmykov Yuri P, *J of Appl Phys*, 113 (2013) 053903.
5 Shibata K, *Materials Trans*, 44 (2003) 1542.
6 Mercey B, Prellier W & Fouchet A, *J Phys Condens Matter*, 15 (2003) 1583.
7 Kammermeier H T, *Doctoral thesis*, University of Duisburg-Essen, (2010).
8 Srinivas K, Rao S M & Reddy P V, *J of Nanoparticle Res*, 13 (2011) 817.
9 Wesselinowa J M & Apostolov A T, *J of Appl Phys*, 107 (2010).
10 Sharma P K, Dutta R K, Pandey A C, Layek S & Verma H C, *J of Magnetism & Magnetic Materials*, 321 (2009).
11 Huang G J, Wang J B, Zhong X L, Zhou G C & Yan H L, *J of Materials Sci*, 42 (2007) 6464.
12 Mandal S K, Das A K & Satpati T K Nath, *J of Appl Phys*, 100 (2006).
13 Schilfgaarde M V & Myrasov M V O N, *Phys Rev B*, 63 (2001) 233205.
14 Stoner E C & Wohlfarth E P, *Phil Trans R Soc Lond A*, 240 (1948) 599.
15 Oogane M, Wakitani T, Yakata S, Yilgin R, Ando Y, Sakuma A & Miyazaki T, *Japan J Appl Phys*, 45 (2006) 3889.
16 Thota S, Dutta T & Kumar J, *J Phys Condens Matter*, 18 (2006) 2473.
17 Anghel J, Thurber A, Tenne D A, Hanna C B & Pun-Noose A, *J Appl Phys*, 107 (2010) 09E314.
18 Ivill M, Pearton S J, Rawal S, Leu L, Sadik P, Das R, Hebard A F, Chisholm M, Budai J D & Norton D P, *New J of Phys*, 10 (2008) 065002.
19 Wanga C, Z Chen, He Y, Li L & Zhang D, *Appl Surface Sci,* 255 (2009) 6881.
20 Liu X, Lin F, Sun L, Cheng W & Ma X, *Appl Phys Lett*, 88 (2006) 062508.
21 Zhang Y B, Liu Q, Sritharan T, Gan C L & Li S, *Appl Phys Lett*, 89 (2006) 042510.
22 Panigrahy B, Aslam M & Bahadur D, *Nanotechnology,* 23 (2012) 115601.
23 Xian F L, Xu L H, Wang X X & Li X Y, *Cryst Res Technol*, 47 (2012) 423.
24 Li B B, Xiu X Q, Zhang R, Xie Z L, Chen Y, Shi Y, Han P & Zheng Y D, *Semiconducting & Insulating Materials*, (2004) 202.
25 Thirion Christophe, Wernsdorfer Wolfgang & Mailly Dominique, *Nature Materials*, 2 (2003) 524.
26 Tannous C & Gieraltowski J, *Eur J Phys*, 29 (2008).
27 Blundell S*, Magnetism in Condensed Matt*, Oxford University Press, 1st edition, (2001).
28 Brown W F, *Micromagnetics*, Wiley Interscience Publishers, New-York, (1963).
29 Bertotti G, *Hysteresis in Magnetism*, Academic Press, London, (1998).
30 Yoon S & Krishnan K M, *J of Appl Phys*, 109 (2011) 07B534.
31 Kikuchi R, *J Appl Phys*, 27 (1956) 1352.
32 Mathias G, *Fundamentals of Magnetism*, Springer Berlin Heidelberg, (2008).
33 Cieniek B, Stefaniuk I & Virt I, *Nukleonika*, 58 (2013) 359.
34 Wibowo J A, Djaja N F & Saleh R, Adv in Materials Phys & Chem, 3 (2013) 48.
35 Saleh R, Prakoso S P & Fishli A, *J of Magnetism & Magnetic Materials,* 324 (2012) 665.
36 Saleh R, Djaja N F & Prakoso S P, *J of Al and Compounds*, 546 (2013) 48.
37 Banwell C N & McCash E M, *Fundamental of Molecular Spectroscopy*, Tata McGraw-Hill, 4th edition, (1993).
38 Jelenski A, Szymczak H & Gutowski M, *Le J De Physique*, 36 (1975)1011.